

NONADIABATIC TRANSITIONS IN MULTIPLE DIMENSIONS*

V. BETZ[†], B. D. GODDARD[‡], AND TIM HURST[§]

Abstract. We consider nonadiabatic transitions in multiple dimensions, which occur when the Born–Oppenheimer approximation breaks down. We present a general, multidimensional algorithm which can be used to accurately and efficiently compute the transmitted wavepacket at an avoided crossing. The algorithm requires only one-level Born–Oppenheimer dynamics and local knowledge of the potential surfaces. Crucially, in contrast to many standard methods in the literature, we compute the whole wavepacket, including its phase, rather than simply the transition probability. We show the excellent agreement with full quantum dynamics for a range of examples in two dimensions. We also demonstrate surprisingly good agreement for a system with a full conical intersection.

Key words. time-dependent Schrödinger equation, nonadiabatic transitions, superadiabatic representations

AMS subject classifications. 35Q40, 81V55

DOI. 10.1137/18M1188756

1. Introduction. Many computations in quantum molecular dynamics rely on the Born–Oppenheimer approximation (BOA) [13], which utilizes the small ratio ε^2 of electronic and reduced nuclear masses to replace the electronic degrees of freedom with *Born–Oppenheimer* potential surfaces. When these surfaces are well separated, the BOA further reduces computational complexity by decoupling the dynamics to individual surfaces.

However, there are many physical examples (see, e.g., [15, 16, 35, 40]) where the Born–Oppenheimer surfaces are not well separated (known as an *avoided crossing*) or even have a full intersection. In these regions, the BOA breaks down, and the coupled dynamics must be considered; when a wavepacket travels over a region where the surfaces are separated by a small but nonvanishing amount, a chemically crucial portion of the wavepacket can move to a different energy level via a *nonadiabatic transition*. The existence of the small parameter ε introduces several challenges when attempting to numerically approximate the dynamics. First, and independently of the existence of an avoided or full crossing, the wavepacket oscillates with frequency $1/\varepsilon$, and hence a very fine computational grid is required. Furthermore, in the region of an avoided crossing, the dynamics produce rapid oscillations and, in turn, cancelations in the wavepacket; the transmitted wavepacket very close to the crossing is $\mathcal{O}(\varepsilon)$, but in the scattering regime the transmission is exponentially small. It is therefore

*Submitted to the journal's Computational Methods in Science and Engineering section May 21, 2018; accepted for publication (in revised form) July 10, 2019; published electronically October 1, 2019.

<https://doi.org/10.1137/18M1188756>

Funding: The third author's research was supported by The Maxwell Institute Graduate School in Analysis and its Applications, a Centre for Doctoral Training funded by the UK Engineering and Physical Sciences Research Council (grant EP/L016508/01), the Scottish Funding Council, Heriot-Watt University, and the University of Edinburgh.

[†]Fachbereich Mathematik, Technische Universität Darmstadt, 64289 Darmstadt, Germany (betz@mathematik.tu-darmstadt.de, <http://www.mathematik.tu-darmstadt.de/~betz/>).

[‡]School of Mathematics and the Maxwell Institute for Mathematical Sciences, University of Edinburgh, Edinburgh, UK, EH9 3FD (b.goddard@ed.ac.uk, <http://www.maths.ed.ac.uk/~bgoddard/>).

[§]Maxwell Institute for Mathematical Sciences, School of Mathematics, University of Edinburgh, Edinburgh, UK, EH9 3FD (t.hurst@sms.ed.ac.uk, <http://www.maxwell.ac.uk/migsaa/people/tim-hurst>).

necessary to travel far from the avoided crossing (in position space) with a small time-step to accurately calculate the phase, size, and shape of the transmitted wavepacket. In order to calculate the exponentially small wavepacket, one must ensure that the absolute errors in a given numerical scheme are also exponentially small, or they will swamp the true result. Finally, the number of gridpoints in the domain increases exponentially as the dimension of the system increases. Thus standard numerical algorithms quickly become computationally intractable.

Many efforts have been made to avoid computational expense by approximating the transmitted wavepacket while avoiding the coupled dynamics. *Surface hopping algorithms* discussed in [41, 33, 37, 29, 39, 23, 34, 36, 17, 18, 31, 4, 3] approximate the transition using classical dynamics, where the *Landau-Zener transition rate* [42, 30] is sometimes used to determine the size of the transmitted wavepacket. This method has enjoyed some success and has been applied to higher dimensional systems (in particular, see [31, 4]). However, the full transmitted quantum wavepacket is not always calculated; phase information is lost, although surface hopping approaches have been considered which try to incorporate phase information [21, 32, 14, 27, 24, 26]. Such information is crucial when considering systems with interference effects, e.g., ones in which the initial wavepacket makes multiple transitions through an avoided crossing. In contrast, in [10, 7], a formula is derived to accurately approximate the full transmitted wavepacket, in one dimension, using only decoupled dynamics. The formula has been applied to a variety of examples with accurate results, including the transmitted wavepacket due to photodissociation of sodium iodide [9].

In this paper, we construct a method to apply the formula derived in [10, 7] to higher dimensional problems. We set up the problem, state assumptions, and give the main result and algorithm in section 2. Our derivation is motivated by the derivation of the formula in one dimension [10], which we outline in section 3 and extend to d dimensions in section 4. In section 5, we create a d -dimensional formula for systems in which, near the avoided crossing, the derivatives of the adiabatic potential surfaces are slowly varying in all but the direction in which the wavepacket is traveling. We then extend this result via a simple algorithm to obtain a general d -dimensional formula. We provide some examples and results in section 6 and note conclusions and future work in section 7.

2. Setup and main results. We consider the evolution of a semiclassical wavepacket $\psi : \mathbb{R}^d \rightarrow \mathbb{C}^2$ at time t , $\psi = (\begin{smallmatrix} \psi_1(\mathbf{x}, t) \\ \psi_2(\mathbf{x}, t) \end{smallmatrix})$, governed by the equation

$$(2.1) \quad i\varepsilon \partial_t \psi(\mathbf{x}, t) = H\psi(\mathbf{x}, t),$$

where ε^2 is the ratio between an electron and the reduced nuclear mass of the molecule, i.e., $\varepsilon \ll 1$ and H is a Hamiltonian operator. This system is derived after a standard rescaling of a full two-level Schrödinger equation involving the kinetic and potential terms between electrons and nuclei, which is given, for example, in [20]. We use the ε -scaled Fourier transform to transform the wavepackets ψ_1, ψ_2 and operators such as H into momentum space.

DEFINITION 2.1. *In d dimensions, the wavepacket $f : \mathbb{R}^d \rightarrow \mathbb{C}$ in scaled momentum space is given using the ε -scaled Fourier transform*

$$(2.2) \quad \widehat{f^\varepsilon}(\mathbf{k}) = \frac{1}{(2\pi\varepsilon)^{d/2}} \int_{\mathbb{R}^d} f(\mathbf{x}) \exp\left(-\frac{i}{\varepsilon} \mathbf{k} \cdot \mathbf{x}\right) d\mathbf{x}.$$

For any (sufficiently nice) function $f : \mathbb{R}^d \rightarrow \mathbb{C} \in L^2(\mathbb{R}^d)$, the ε -scaled Fourier

transform \widehat{A}^ε of an operator A is given by

$$(2.3) \quad \widehat{A}^\varepsilon \widehat{f}^\varepsilon(\mathbf{k}, t) := \widehat{Af}^\varepsilon(\mathbf{k}, t) = \frac{1}{(2\pi\varepsilon)^{d/2}} \int_{\mathbb{R}^d} Af(\mathbf{x}, t) \exp\left(-\frac{i}{\varepsilon}\mathbf{k} \cdot \mathbf{x}\right) d\mathbf{x}.$$

We also define the Weyl quantization [2] in multiple dimensions, which is used throughout this paper.

DEFINITION 2.2. *For a symbol $H(\varepsilon, \mathbf{p}, \mathbf{q})$, given a test function ψ , we define the Weyl quantization of H by*

$$(2.4) \quad (\mathcal{W}_\varepsilon H\psi)(\mathbf{x}) = \frac{1}{(2\pi\varepsilon)^d} \int_{\mathbb{R}^{2d}} d\mathbf{\xi} d\mathbf{y} H\left(\varepsilon, \mathbf{\xi}, \frac{1}{2}(\mathbf{x} + \mathbf{y})\right) e^{\frac{i}{\varepsilon}(\mathbf{\xi} \cdot (\mathbf{x} - \mathbf{y}))} \psi(\mathbf{y}).$$

The Hamiltonian in (2.1) is given by [7]

$$(2.5) \quad H(\mathbf{x}) = -\frac{\varepsilon^2}{2} \nabla_{\mathbf{x}}^2 I + V(\mathbf{x}) + d(\mathbf{x}) I,$$

where

$$(2.6) \quad V(\mathbf{x}) = \begin{pmatrix} Z(\mathbf{x}) & X(\mathbf{x}) \\ X(\mathbf{x}) & -Z(\mathbf{x}) \end{pmatrix}$$

and $d(\mathbf{x})$ is the part of the potential operator with nonzero trace. In general, $V(\mathbf{x})$ can be given by a Hermitian matrix, but as noted in [5], any Hermitian $V(\mathbf{x})$ can be transformed into real symmetric form. This is known as the *adiabatic representation* of the system. We define $V_1 = Z(\mathbf{x}) + d(\mathbf{x})$ and $V_2 = -Z(\mathbf{x}) + d(\mathbf{x})$ as the two *adiabatic potentials*, with the *adiabatic coupling element* as the off-diagonal element $V_{12} = X(\mathbf{x})$. It is useful to define $\theta(\mathbf{x}) = \tan^{-1}\left(\frac{X(\mathbf{x})}{Z(\mathbf{x})}\right)$, so that we can write the polar decomposition of (2.5):

$$(2.7) \quad \cos(\theta(\mathbf{x})) = \frac{Z(\mathbf{x})}{\sqrt{X(\mathbf{x})^2 + Z(\mathbf{x})^2}}, \quad \sin(\theta(\mathbf{x})) = \frac{X(\mathbf{x})}{\sqrt{X(\mathbf{x})^2 + Z(\mathbf{x})^2}}.$$

Then, defining $\rho(\mathbf{x}) = \sqrt{X(\mathbf{x})^2 + Z(\mathbf{x})^2}$, we have

$$(2.8) \quad V(\mathbf{x}) = \rho(\mathbf{x}) \begin{pmatrix} \cos(\theta(\mathbf{x})) & \sin(\theta(\mathbf{x})) \\ \sin(\theta(\mathbf{x})) & -\cos(\theta(\mathbf{x})) \end{pmatrix}.$$

Consider the unitary matrix U_0 which diagonalizes the potential operator $V(\mathbf{x})$:

$$(2.9) \quad U_0(\mathbf{x}) = \begin{pmatrix} \cos\left(\frac{\theta(\mathbf{x})}{2}\right) & \sin\left(\frac{\theta(\mathbf{x})}{2}\right) \\ \sin\left(\frac{\theta(\mathbf{x})}{2}\right) & -\cos\left(\frac{\theta(\mathbf{x})}{2}\right) \end{pmatrix}.$$

If we define $\psi_0(\mathbf{x}, t) = \begin{pmatrix} \psi_+^{+}(\mathbf{x}, t) \\ \psi_-^{+}(\mathbf{x}, t) \end{pmatrix} = U_0(\mathbf{x})\psi(\mathbf{x}, t)$, then we arrive at the *adiabatic Schrödinger equation*

$$(2.10) \quad i\varepsilon \partial_t \psi_0(\mathbf{x}, t) = H_0 \psi_0(\mathbf{x}, t).$$

Here $H_0 = U_0 H U_0^{-1}$ is given by

$$(2.11) \quad H_0(\mathbf{x}) = -\frac{\varepsilon^2}{2} \nabla_{\mathbf{x}}^2 \mathbf{I} + \begin{pmatrix} \rho(\mathbf{x}) + d(\mathbf{x}) + \varepsilon^2 \frac{\|\nabla_{\mathbf{x}} \theta(\mathbf{x})\|^2}{8} & -\varepsilon \frac{\nabla_{\mathbf{x}} \theta(\mathbf{x})}{2} \cdot (\varepsilon \nabla_{\mathbf{x}}) - \varepsilon^2 \frac{\nabla_{\mathbf{x}}^2 \theta(\mathbf{x})}{4} \\ \varepsilon \frac{\nabla_{\mathbf{x}} \theta(\mathbf{x})}{2} \cdot (\varepsilon \nabla_{\mathbf{x}}) + \varepsilon^2 \frac{\nabla_{\mathbf{x}}^2 \theta(\mathbf{x})}{4} & -\rho(\mathbf{x}) + d(\mathbf{x}) + \varepsilon^2 \frac{\|\nabla_{\mathbf{x}} \theta(\mathbf{x})\|^2}{8} \end{pmatrix}.$$

The *adiabatic potential surfaces* are given by the diagonal entries of the adiabatic potential matrix to leading order,

$$(2.12) \quad V_U(\mathbf{x}) = \rho(\mathbf{x}) + d(\mathbf{x}), \quad V_L(\mathbf{x}) = -\rho(\mathbf{x}) + d(\mathbf{x}),$$

where V_U is the upper adiabatic potential surface, and V_L is the lower adiabatic potential surface. The off-diagonal entries of (2.12) are coupling terms, which are negligible when the two adiabatic surfaces are well separated. An avoided crossing occurs when two adiabatic surfaces become close to one another, and the coupling terms have a nonnegligible effect. Note that, as we are considering semiclassical wavepackets, derivatives are of order $1/\varepsilon$, and hence the leading order off-diagonal elements are of order ε .

For a more precise definition of an avoided crossing, we direct the reader to [22] (although it should be noted that the precise meaning of an avoided crossing does vary in the literature), but for the purposes of this paper we will work with a definition of an avoided crossing with respect to the wavepacket. We define the *center of mass* of the wavepacket ψ^\pm at time t by

$$(2.13) \quad \mathbf{x}_{\text{COM}}(t) = \frac{\int_{\mathbb{R}^n} d\mathbf{x} \mathbf{x} |\psi^\pm(\mathbf{x}, t)|^2}{\int_{\mathbb{R}^n} d\mathbf{x} |\psi^\pm(\mathbf{x}, t)|^2}$$

and the *center of momentum* of ψ^\pm by

$$(2.14) \quad \mathbf{p}_{\text{COM}}(t) = \frac{\int_{\mathbb{R}^n} d\mathbf{p} \mathbf{p} |\widehat{\psi^\pm}^\varepsilon(\mathbf{p}, t)|^2}{\int_{\mathbb{R}^n} d\mathbf{p} |\widehat{\psi^\pm}^\varepsilon(\mathbf{p}, t)|^2}.$$

DEFINITION 2.3. Let V_U and V_L be the adiabatic surfaces defined in (2.12) such that $V_U(\mathbf{x}) - V_L(\mathbf{x}) = 2\rho(\mathbf{x})$. A wavepacket ψ^\pm on the upper/lower level is said to reach an avoided crossing at time t when $\rho(\mathbf{x}_{\text{COM}}(t))$ reaches a local minimum of ρ along its trajectory. Furthermore, we say that the avoided crossing is tilted when, near the avoided crossing, the nonsymmetric part $d(\mathbf{x})$ of V_U and V_L can be written as $d(\mathbf{x}) = \boldsymbol{\lambda} \cdot \mathbf{x} + \mathcal{O}(\|\mathbf{x}\|^2)$, where $\boldsymbol{\lambda}$ is nonzero in the direction $\mathbf{p}_{\text{COM}}(t)$.

We note that, at an avoided crossing, the derivative couplings in (2.11) are nonnegligible, and it is in such regions that we expect the transitions between the adiabatic states to occur. In the following, we consider only cases in which the avoided crossing is of dimension zero, due either to the nature of the potential energy surfaces or the path of the wavepacket. In cases where the dimension is higher, for example, when the wavepacket travels along a “seam” of avoided crossings, we expect the method to break down. For the case of “tilted” crossings in one dimension, we refer the reader to [8] and note that we will soon make the assumption that $\|\boldsymbol{\lambda}\|$ is small in the direction of \mathbf{p}_{COM} and thus not treat the “tilted” case here.

We will assume that the initial wavepacket is purely on the upper level, $\psi^0(\mathbf{x}) = (\begin{smallmatrix} \psi^{0,+}(\mathbf{x}) \\ 0 \end{smallmatrix})$, and, without loss of generality, that the center of mass of the wavepacket in position space reaches an avoided crossing of height 2δ at position \mathbf{x}_0 at time t_{ac} and is moving in the direction of \mathbf{q}_1 . The adiabatic representation approximates the wavepacket transmitted through an avoided crossing to leading order by the perturbative solution [38]

$$(2.15) \quad \psi_0^-(\mathbf{x}, t) = -i\varepsilon \int_{-\infty}^t e^{-\frac{i}{\varepsilon}(t-s)H^-(\mathbf{x})} \kappa_1^-(\mathbf{x}) \cdot (\varepsilon \partial_{\mathbf{x}}) e^{-\frac{i}{\varepsilon}sH^+(\mathbf{x})} \psi^{0,+}(\mathbf{x}) ds,$$

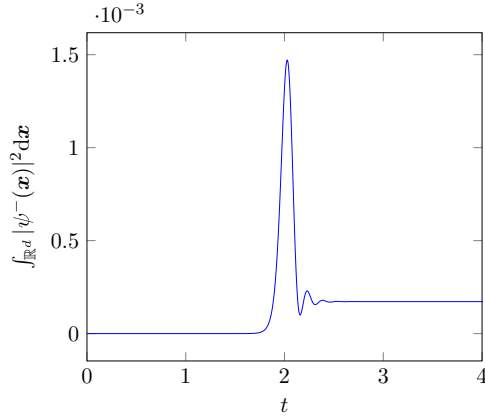


FIG. 1. The total mass of wavepacket $\psi^-(\mathbf{x})$ on the lower potential surface against time t for the system described in Example 6.1 with parameters in (6.7). The center of mass of the wavepacket reaches the avoided crossing at $t = 2$.

where

$$(2.16) \quad H^\pm(\mathbf{x}) = -\frac{\varepsilon^2}{2}\nabla_{\mathbf{x}}^2 \pm \rho(\mathbf{x}) + d(\mathbf{x}), \quad \kappa_1^\pm(\mathbf{x}) = \pm \frac{\partial_{\mathbf{x}}\theta(\mathbf{x})}{2}.$$

The perturbative solution in the adiabatic representation does not offer much explanation as to the properties of the transmitted wavepacket. For instance, the constructed wavepacket at first looks to be $\mathcal{O}(\varepsilon)$. However, due to the adiabatic coupling operator κ_1^\pm , fast oscillations and cancelations between upper and lower transmissions occur near the avoided crossing, so that far from the crossing in position space the transmitted wavepacket is much smaller than the transition at the crossing point (Figure 1). For this reason, the transmitted wavepacket is better approximated using the perturbative solution from the n th *superadiabatic* representation [10] for some optimal choice of n . The n th superadiabatic representation is produced by creating and applying unitary *pseudodifferential* operators U_n , such that the off-diagonal elements of the potential operator have prefactor ε^{n+1} , and the diagonal elements are the same to leading order as in the adiabatic representation. Existence of such operators is discussed in [10]. The Hamiltonian H_n in the n th superadiabatic representation is given by

$$(2.17) \quad H_n(\mathbf{x}) = -\frac{\varepsilon^2}{2}\nabla_{\mathbf{x}}^2 \mathbf{I} + \begin{pmatrix} \rho(\mathbf{x}) + d(\mathbf{x}) + \mathcal{O}(\varepsilon^2) & \varepsilon^{n+1} K_{n+1}^+ \\ \varepsilon^{n+1} K_{n+1}^- & -\rho(\mathbf{x}) + d(\mathbf{x}) + \mathcal{O}(\varepsilon^2) \end{pmatrix}$$

for some pseudodifferential coupling operators K_{n+1}^\pm , which are of order one. The perturbative solution in the n th superadiabatic representation is then given by

$$(2.18) \quad \psi_n^-(\mathbf{x}, t) = -i\varepsilon^n \int_{-\infty}^t e^{-\frac{i}{\varepsilon}(t-s)H^-(\mathbf{x})} K_{n+1}^-(\mathbf{x}) e^{-\frac{i}{\varepsilon}sH^+(\mathbf{x})} \psi^{0,+}(\mathbf{x}) ds.$$

Direct computation of the pseudodifferential operators K_{n+1} and U_n is recursive in n (see section 4), and leads to very complex operators, and so we cannot produce a practical numerical scheme directly using superadiabatic representations. However, we will use superadiabatic representations to construct a simple and accurate algorithm.

In [7], where a formula approximating the transmitted wavepacket in one dimension is constructed, five assumptions are made:

- (A1) The avoided crossing is “flat”; i.e., $\|\boldsymbol{\lambda}\|$ in Definition 2.3 is small (in the direction of $\mathbf{p}_{\text{COM}}(t_{\text{ac}})$) compared to the energy gap, 2δ . This approximation can be removed in one dimension [8], but the resulting algorithm is more complicated; we will pursue the multidimensional version of this in future work.
- (A2) The momentum of the wavepacket near the avoided crossing is sufficiently large. Furthermore, by a coordinate rotation we can assume without loss of generality that the momentum is concentrated in the first dimension. This allows the quantum symbol of the coupling operator K_{n+1} to be approximated by its highest order polynomial term, as discussed in section 4.
- (A3) The first order Taylor approximation of the adiabatic (Born–Oppenheimer) energy surfaces near \mathbf{x}_0 leads to a dynamics that is a good approximation of the true dynamics near \mathbf{x}_0 ; i.e., we can write the adiabatic propagators near the avoided crossing as

$$(2.19) \quad H^\pm \approx -\frac{\varepsilon^2}{2} \nabla_{\mathbf{x}}^2 \pm \delta + \boldsymbol{\lambda} \cdot \mathbf{x}.$$

- (A4) The width of the wavepacket is $\mathcal{O}(\varepsilon)$. For the one dimensional case, it has been shown [9] that, by the linearity of the Schrödinger equation, we can consider wider wavepackets through a slicing method. We expect this to also hold in higher dimensions.

- (A5) The functions ρ and θ are analytic in a strip containing the real axis.

In the multidimensional derivation, we will make one additional assumption:

- (A6) The adiabatic potential surfaces near the avoided crossing point vary slowly in all but the direction of $\mathbf{p}_{\text{COM}}(t_{\text{ac}})$.

We are now ready to state the main result of this paper. Under the assumptions (A2) to (A6), we approximate the transmitted wavepacket at the avoided crossing point using the formula

$$(2.20) \quad \widehat{\psi^{-}}^{\varepsilon}(\mathbf{k}, t) = e^{-\frac{i}{\varepsilon}t\widehat{H}^{-\varepsilon}} \frac{\nu(k_1) + k_1}{2|\nu(k_1)|} e^{-\frac{i}{\varepsilon}(k_1 - \nu(k_1))(x_0 + \frac{\tau_r}{2\delta})} e^{-\frac{\tau_c}{2\delta\varepsilon}|k_1 - \nu(k_1)|} \\ \times \chi_{k_1^2 > 4\delta} \widehat{\phi^{+}}^{\varepsilon}(\nu(k_1), k_2, \dots, k_d),$$

where ξ , ν , τ_c , and τ_r are the d -dimensional analogues of those quantities defined in one dimension in (D1) to (D4) and are discussed in sections 4 and 5. Here, as described precisely in Algorithm 2.4 below, ϕ^{+} is the wavepacket on the upper level at the avoided crossing.

We outline the method through which (2.20) may be used to compute the transmitted wavepacket using only one-level dynamics via the following algorithm and two dimensional diagrams available in Figure SM1 of the supplementary materials, linked from the main article webpage.

ALGORITHM 2.4.

- (B1) Begin with an initial wave packet $\psi^{0,+}(\mathbf{x})$ on the upper adiabatic energy surface, far from the crossing in position space, with momentum such that $\rho(\mathbf{x}_{\text{COM}}(t))$ will attain a minimum value (Figure SM1a).
- (B2) Evolve $\psi^{0,+}$ on the upper level, i.e., under the BOA, until its center of mass

reaches a local minimum at time t_{ac} . Define

$$(2.21) \quad \phi^+(\mathbf{x}) := e^{-\frac{i}{\varepsilon}t_{\text{ac}}H^+(\mathbf{x})}\psi^{0,+}(\mathbf{x}).$$

- (B3) Divide up the full d -dimensional space into d -dimensional strips parallel to $\mathbf{p}_{\text{COM}}(t_{\text{ac}})$. The width of the strips in all directions perpendicular to $\mathbf{p}_{\text{COM}}(t_{\text{ac}})$ should be of the order of the width of the transition region (along $\mathbf{p}_{\text{COM}}(t_{\text{ac}})$) in the optimal superadiabatic basis. In practice, we restrict these strips to the region of space where the wavepacket has significant mass.
- (B4) On each strip, replace the true potential energy matrix by an approximation that is flat perpendicular to the direction of $\mathbf{p}_{\text{COM}}(t_{\text{ac}})$. In practice, we take the potential along $\mathbf{p}_{\text{COM}}(t_{\text{ac}})$ in the middle of the strip and replicate it in the directions perpendicular to $\mathbf{p}_{\text{COM}}(t_{\text{ac}})$. Note, in particular, that the new potential may be different for each strip.
- (B5) Compute the transmitted wavepacket on the lower level for each strip by applying the formula (2.20) along \mathbf{p}_{COM} (Figure SM1c), and sum them together: $\widehat{\psi}^-(\mathbf{k}, t_{\text{ac}}) = \sum_{j=1}^n \widehat{\psi}_j^-(\mathbf{k}, t_{\text{ac}})$.
- (B6) Evolve the transmitted wavepacket away from the avoided crossing on the lower level, say to time $t_{\text{ac}} + s$, using the BOA (Figure SM1e): $\widehat{\psi}^-(\mathbf{k}, t_{\text{ac}} + s) = e^{-\frac{i}{\varepsilon}s\widehat{H}^-\varepsilon} \widehat{\psi}^-(\mathbf{k}, t_{\text{ac}})$.

To summarize, we have derived an algorithm for approximating the transmitted wavepacket for an avoided crossing in any dimension, which only requires one-level dynamics, and local information about the adiabatic electronic surfaces, i.e., δ and τ^{cz} . The dependence on the n th superadiabatic representation is also removed due to cancelations in the derivation. This seems peculiar to the case where (A1) applies and is not expected to be true in general. A similar method can be used to determine transmitted wavepackets from lower to upper levels. We note that when the dimension of the system is large, we still require a high dimensional discretization for simulation of the one-level dynamics. However, methods (see, e.g., [28]) which improve performance of one-level dynamics can be applied to significantly reduce computational cost. In the following section, we derive Algorithm 2.4 and provide numerical examples. We note that for a particular asymptotic limit in one dimension, error bounds have been constructed for this approximation [10], but for general $\mathbf{p}_{\text{COM}}, \varepsilon$ only empirical estimates are available.

3. Motivation: Approximating the transmitted wavepacket in one dimension. The formula is derived in one dimension using the superadiabatic perturbative solution (2.18) by

- (C1) finding algebraic recursive differential equations to calculate the quantum symbol κ_{n+1}^\pm , where K_{n+1}^\pm is the Weyl quantization of κ_{n+1}^\pm ;
- (C2) introducing by a change of variables $\tilde{\kappa}^\pm(\tau(q)) = \kappa_{n+1}^\pm(q)$, where

$$(3.1) \quad \tau(q) = 2 \int_0^q \rho(r) \, dr$$

(which is the *natural scale* discussed in [5]), and then approximating $\tilde{\kappa}_{n+1}^\pm$ in an analogous way to the time-adiabatic case in [11];

- (C3) applying the Avron–Herbst formula [1] to $H^\pm \approx \frac{\varepsilon^2}{2} \partial_x^2 \pm \delta + \lambda x$ by using (A3); and

- (C4) applying a stationary phase argument (with small λ) to evaluate the remaining integral.

Following this derivation leads to an approximation of the transmitted wavepacket in scaled momentum space, far from the avoided crossing in momentum space:

(3.2)

$$\widehat{\psi}^-(k, t) = e^{-\frac{i}{\varepsilon}t\widehat{H}^-\varepsilon} \frac{\nu(k) + k}{2|\nu(k)|} e^{-\frac{i}{\varepsilon}(k - \nu(k))(x_0 + \frac{\tau_r}{2\delta})} e^{-\frac{\tau_c}{2\delta\varepsilon}|k - \nu(k)|} \chi_{k^2 > 4\delta} \widehat{\phi}^+(\nu(k)),$$

where the following hold:

- (D1) The indicator function $\chi_{k^2 > 4\delta}$ (which is one when $k^2 > 4\delta$ and zero otherwise) relates to (classical) energy conservation: kinetic energy from the potential energy difference between two levels must be gained by the wavepacket.
- (D2) The dependence on the n th superadiabatic representation is removed during the formula derivation.
- (D3) $\nu(k) = \text{sgn}(k)(\sqrt{k^2 - 4\delta})$, the initial momentum a classical particle would need to have momentum k after falling down a potential energy difference of 2δ , i.e., the distance between the potential surfaces at the avoided crossing, which shifts the wavepacket in momentum space. This arises naturally; it is often enforced in surface hopping algorithms.
- (D4) $\tau^{cz} := \tau_r + i\tau_c = 2 \int_0^{q^{cz}} \rho(q) dq$, where $q^{cz} \in \mathbb{C}$ is the closest value to the local minimum of ρ such that $\rho(q^{cz}) = 0$, when ρ is extended to the complex plane. The prefactor $e^{-\frac{\tau_c}{2\delta\varepsilon}|\nu(k)-k|}$ determines the size of the transmitted wavepacket. In [20], we show that under appropriate approximations of the momentum and potential surfaces, this prefactor is comparable to the Landau–Zener transition prefactor used in surface hopping algorithms such as in [4]. An additional change in phase occurs due to τ_r , which is present when the potential is not symmetric about the avoided crossing.

The constructed formula (3.2) allows us to approximate the size and shape of the transmitted wave packet due to an avoided crossing and avoid computing expensive coupled dynamics. The method for applying the algorithm is as follows.

ALGORITHM 3.1 (one dimensional version of Algorithm 2.4).

- (E1) Begin with an initial wave packet ψ_0^+ on the upper adiabatic energy surface, far from the crossing in position space, with momentum such that the wave packet will cross the minimum of ρ (Figure 2a).
- (E2) Evolve ψ_0^+ according to the BOA on the upper adiabatic level until the center of mass is at the avoided crossing at time t_{ac} (Figure 2b):

$$(3.3) \quad \phi^+(x) := e^{-\frac{i}{\varepsilon}t_{ac}H^+(x)}\psi_0^{0,+}(x).$$

- (E3) Apply the one dimensional formula to the ε -Fourier transform of the wave packet at the crossing (Figure 2c):

(3.4)

$$\widehat{\psi}^-(k, t_{ac}) = \frac{\nu(k) + k}{2|\nu(k)|} e^{-\frac{i}{\varepsilon}(k - \nu(k))(x_0 + \frac{\tau_r}{2\delta})} e^{-\frac{\tau_c}{2\delta\varepsilon}|k - \nu(k)|} \chi_{k^2 > 4\delta} \widehat{\phi}^+(\nu(k)).$$

- (E4) Evolve the transmitted wave packet far enough away from the crossing in position space, say to time $t_{ac} + s$, using the BOA (Figure 2d): $\widehat{\psi}^-(x, t_{ac} + s) = e^{-\frac{i}{\varepsilon}s\widehat{H}^-\varepsilon} \widehat{\psi}^-(x, t_{ac})$.

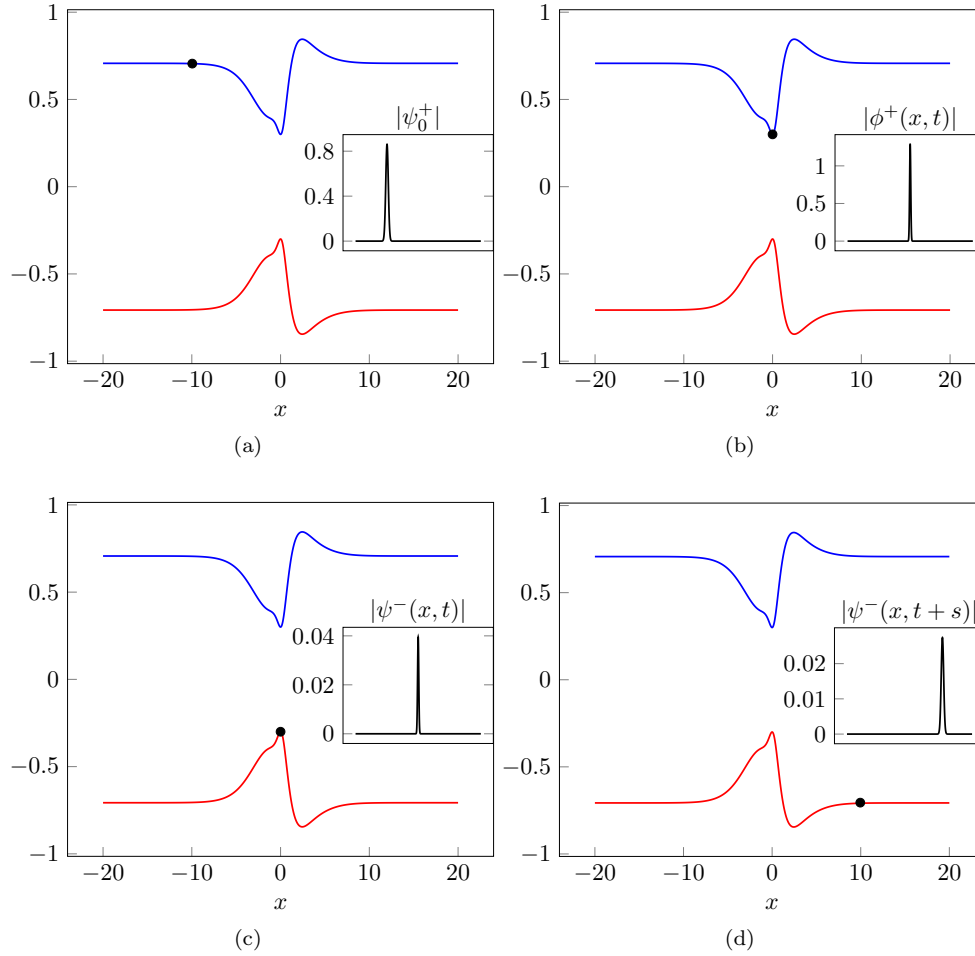


FIG. 2. Application of the one dimensional formula for a particular system discussed in [7]. The center of mass of the associated wavepacket (inset) is represented by a black point on either the upper (blue) and lower (red) adiabatic potential surfaces.

Applications of the one dimensional formula have been widely successful on a variety of examples. In addition to the sodium iodide example [9] already mentioned, tilted avoided crossings have been examined, and a formula has been developed which in contrast is dependent on n . The formula has also been successfully applied to model interference effects in multiple transitions [20].

Finally, the above derivation can also be modified for reverse transitions (from lower to upper surface). If we consider an initial wavepacket ψ_0^- far from the avoided crossing in position space on the lower energy level, the above algorithm can be applied analogously, where to approximate the wavepacket transmitted to the upper level, (3.4) is replaced by

$$(3.5) \quad \widehat{\psi}^+(k, t_{ac}) = \frac{\tilde{\nu}(k) + k}{2|\tilde{\nu}(k)|} e^{-\frac{i}{\varepsilon}(k - \tilde{\nu}(k))(x_0 + \frac{\tau_c}{2\delta})} e^{-\frac{\tau_c}{2\delta\varepsilon}|k - \tilde{\nu}(k)|} \widehat{\phi}^-(\tilde{\nu}(k), t_{ac}),$$

where $\tilde{\nu}(k) = \text{sgn}(k)\sqrt{k^2 + 4\delta}$ contributes a loss of momentum due to the potential

energy difference between the two surfaces.

4. Coupling operators in higher dimensions. The first step in deriving (3.2) in [10] was to approximate the superadiabatic coupling operators K_{n+1}^\pm . We now consider these operators in higher dimensions. We restrict the calculations here to two dimensions for clarity, but they can easily be adapted to d dimensions.

LEMMA 4.1. *In two dimensions, κ_{n+1}^\pm is given by*

$$(4.1) \quad \kappa_{n+1}^\pm(\mathbf{p}, \mathbf{q}) = -2\rho(\mathbf{q})(x_{n+1}(\mathbf{p}, \mathbf{q}) \pm y_{n+1}(\mathbf{p}, \mathbf{q})),$$

where $x_{n+1}(\mathbf{p}, \mathbf{q}), y_{n+1}(\mathbf{p}, \mathbf{q})$ are given by the following algebraic recursive differential equations (where we omit the arguments of symbols to ease notation):

$$(4.2) \quad x_1 = z_1 = w_1 = 0, \quad y_1 = -\frac{i}{4\rho}(\mathbf{p} \cdot \nabla_{\mathbf{q}} \theta)$$

and

$$(4.3) \quad y_n = 0, \quad n \text{ even}, \quad x_n = z_n = w_n = 0, \quad n \text{ odd},$$

where $\rho = \rho(\mathbf{q})$. For n odd, we have

$$(4.4) \quad x_{n+1} = -\frac{1}{2\rho} \left[\frac{1}{i}(\mathbf{p} \cdot \nabla_{\mathbf{q}} y_n) - 2 \sum_{j=1}^n \frac{1}{(2i)^j j!} \sum_{|\alpha|=j} \partial_{\mathbf{p}}^\alpha (b_\alpha z_{n+1-j} - a_\alpha x_{n+1-j}) \right],$$

and for n even,

$$(4.5) \quad y_{n+1} = -\frac{1}{2\rho} \left[\frac{1}{i}((\mathbf{p} \cdot \nabla_{\mathbf{q}} x_n) - z_n(\mathbf{p} \cdot \nabla_{\mathbf{q}} \theta)) - 2 \sum_{j=1}^n \frac{1}{(2i)^j j!} \sum_{|\alpha|=j} \partial_{\mathbf{p}}^\alpha (-a_\alpha y_{n+1-j} + b_\alpha w_{n+1-j}) \right],$$

$$(4.6) \quad \frac{1}{i}((\mathbf{p} \cdot \nabla_{\mathbf{q}} z_n) - x_n(\mathbf{p} \cdot \nabla_{\mathbf{q}} \theta)) = \sum_{j=1}^n \frac{1}{(2i)^j j!} \sum_{|\alpha|=j} \partial_{\mathbf{p}}^\alpha (b_\alpha y_{n+1-j} + a_\alpha w_{n+1-j}),$$

$$(4.7) \quad \frac{1}{i}(\mathbf{p} \cdot \nabla_{\mathbf{q}} w_n) = 2 \sum_{j=1}^n \frac{1}{(2i)^j j!} \sum_{|\alpha|=j} \partial_{\mathbf{p}}^\alpha (a_\alpha z_{n+1-j} + b_\alpha x_{n+1-j}),$$

where $\alpha = (\alpha_1, \alpha_2)$, $\partial_{\mathbf{p}}^\alpha = \partial_{p_1}^{\alpha_1} \partial_{p_2}^{\alpha_2}$ and $a_\alpha = a_\alpha(\mathbf{q})$, $b_\alpha = b_\alpha(\mathbf{q})$ depend only on \mathbf{q} and are given by the recursions

$$\begin{aligned} a_0 &= \rho(\mathbf{q}), & b_0 &= 0, \\ a_{(\alpha_1+1, \alpha_2)} &= \partial_{q_1} a_{(\alpha_1, \alpha_2)} + (\partial_{q_1} \theta) b_{(\alpha_1, \alpha_2)}, & b_{(\alpha_1+1, \alpha_2)} &= \partial_{q_1} b_{(\alpha_1, \alpha_2)} - (\partial_{q_1} \theta) a_{(\alpha_1, \alpha_2)}, \\ a_{(\alpha_1, \alpha_2+1)} &= \partial_{q_2} a_{(\alpha_1, \alpha_2)} + (\partial_{q_2} \theta) b_{(\alpha_1, \alpha_2)}, & b_{(\alpha_1, \alpha_2+1)} &= \partial_{q_2} b_{(\alpha_1, \alpha_2)} - (\partial_{q_2} \theta) a_{(\alpha_1, \alpha_2)}. \end{aligned}$$

Proof. The method is a straightforward extension of [10, sections 2 and 3]; in particular, we direct the reader to Proposition 3.3 (page 3564). \square

The result of Lemma 4.1 shows that x_n, y_n, z_n, w_n can be written as polynomials in \mathbf{p} of order n , as the recursive definitions involve finite products, derivatives, and sums of the initial x_0, y_0, z_0, w_0 , which are polynomials in \mathbf{p} . We therefore write

$$(4.8) \quad x_n(\mathbf{p}, \mathbf{q}) = \sum_{m=0}^n \sum_{k=0}^m p_1^k p_2^{m-k} x_n^{k,m-k}(\mathbf{q})$$

for some $x_n^{k,m-k}(\mathbf{q})$, and similarly for y_n, z_n, w_n . For a given j , we write $\alpha_j = (\alpha, j-\alpha)$ for each $\alpha \leq j$.

Consider, for example,

$$\partial_{\mathbf{p}}^{\alpha_j} x_{n+1-j} = \sum_{m=0}^{n+1-j} \sum_{k=0}^m (\partial_{p_1}^\alpha p_1^k) (\partial_{p_2}^{j-\alpha} p_2^{m-k}) x_{n+1-j}^{k,m-k}(\mathbf{q}),$$

where by a direct calculation

$$(4.9) \quad \partial_{\mathbf{p}}^{\alpha_j} p_1^k p_2^{m-k} = \begin{cases} \frac{k!}{(m-k)!} \frac{(m-k)!}{(m-k-j+\alpha)!} p_1^{k-\alpha} p_2^{m-k-j+\alpha}, & k \geq \alpha \text{ and } m \geq j, \\ 0 & \text{otherwise.} \end{cases}$$

Therefore,

$$\partial_{\mathbf{p}}^{\alpha_j} x_{n+1-j} = \sum_{m=j}^{n+1-j} \sum_{k=\alpha}^{m-\alpha+j} \frac{k!}{(k-\alpha)!} \frac{(m-k)!}{(m-k-j+\alpha)!} p_1^{k-\alpha} p_2^{m-k-j+\alpha} x_{n+1-j}^{k,m-k}(\mathbf{q}),$$

so that

$$(4.10) \quad \mathcal{A}(\mathbf{p}, \mathbf{q}) := \sum_{j=1}^n \frac{1}{(2i)^j j!} \sum_{\alpha=0}^j a_{\alpha_j} \partial_{p_1}^\alpha \partial_{p_2}^{j-\alpha} x_{n+1-j}(\mathbf{p}, \mathbf{q})$$

can be rewritten as

$$\sum_{j=1}^n \frac{1}{(2i)^j j!} \sum_{\alpha=0}^j a_{\alpha_j} \sum_{m=j}^{n+1-j} \sum_{k=\alpha}^{m+\alpha-j} \frac{k!}{(k-\alpha)!} \frac{(m-k)!}{(m-k-j+\alpha)!} p_1^{k-\alpha} p_2^{m-k-j+\alpha} x_{n+1-j}^{k,m-k}(\mathbf{q}).$$

We now want to extract p_1 and p_2 from the final two summations, so that we can compare coefficients on either side of the results of Lemma 4.1 to construct recursive equations for $x_n^{A,B}$ for $A+B < n$. Consider terms where $j > \frac{n+1}{2}$. By the limits of the third summand, we find that $m > \frac{n+1}{2}$, and that $m < \frac{n+1}{2}$, a contradiction. Therefore, we restrict the limits of the first summand. Defining $b = k - \alpha$ and $c = m - j$, we find that

$$\mathcal{A} = \sum_{j=1}^{\lfloor \frac{n+1}{2} \rfloor} \sum_{\alpha=0}^j \sum_{c=0}^{n+1-2j} \sum_{b=0}^c \frac{a_{\alpha_j} (b+\alpha)! ((c+j) - (b+\alpha))!}{(2i)^j j! b! (c-b)!} p_1^b p_2^{c-b} x_{n+1-j}^{b+\alpha, (c+j)-(b+\alpha)}(\mathbf{q}).$$

We now want to switch the order of summation. We note that, for an arbitrary \mathcal{B} ,

$$\sum_{j=1}^{\lfloor \frac{n+1}{2} \rfloor} \sum_{c=0}^{n+1-2j} \mathcal{B}_{c,j} = \sum_{c=0}^{n+1} \sum_{j=1}^{\lfloor \frac{c}{2} \rfloor} \mathcal{B}_{n+1-c,j},$$

which can be shown directly (note that the terms where $c = 0, c = 1$ are zero). Using this, we finally have that

$$(4.11) \quad \mathcal{A} = \sum_{c=0}^{n+1} \sum_{b=0}^{n+1-c} p_1^b p_2^{n+1-c-b} \\ \times \sum_{j=1}^{\lfloor \frac{c}{2} \rfloor} \sum_{\alpha=0}^j \frac{a_{\alpha_j} (b+\alpha)! (n+1-c+j-b-\alpha)!}{(2i)^j j! b! (n+1-c-b)!} x_{n+1-j}^{b+\alpha, (n+1-c+j)-(b+\alpha)}(\mathbf{q}).$$

Importantly, p_1 and p_2 have been extracted from two of the summations. Note that (4.11) reduces to the one dimensional result in [10] for p_2 and p_1 by taking $b = 0$ and $\alpha = 0$, or $j - \alpha = 0$ and $n + 1 - c - b = 0$, respectively. We then obtain the following result.

PROPOSITION 4.2. *The coefficients $x_n^{A,B}(\mathbf{q})$ to $w_n^{A,B}(\mathbf{q})$ are determined by the following algebraic differential recursive equations. We have (omitting arguments of symbols for ease of notation)*

$$(4.12) \quad x_1^{A,B} = z_1^{A,B} = w_1^{A,B} = 0, \quad A + B \in \{0, 1\},$$

$$(4.13) \quad y_1^{0,0} = y_1^{1,1} = 0, \quad y_1^{1,0} = -\frac{i}{4\rho} \partial_{q_1} \theta, \quad y_1^{0,1} = -\frac{i}{4\rho} \partial_{q_2} \theta.$$

Further, when n is odd,

$$(4.14) \quad x_{n+1}^{A,B} = -\frac{1}{2\rho} \left[\frac{1}{i} (\partial_{q_1} y_n^{A-1,B} + \partial_{q_2} y_n^{A,B-1}) - 2 \sum_{j=1}^{\lfloor \frac{n+1-(A+B)}{2} \rfloor} \sum_{\alpha=0}^j \frac{1}{(2i)^j j!} \right. \\ \left. \times \frac{(A+\alpha)! (B+j-\alpha)!}{A! B!} \left(b_{\alpha_j} z_{n+1-j}^{A+\alpha, B+j-\alpha} - a_{\alpha_j} x_{n+1-j}^{A+\alpha, B+j-\alpha} \right) \right].$$

When n is even, we have

$$(4.15) \quad y_{n+1}^{A,B} = -\frac{1}{2\rho} \left[\frac{1}{i} ((\partial_{q_1} x_n^{A-1,B} + \partial_{q_2} x_n^{A,B-1}) - (z_n^{A-1,B} \partial_{q_1} \theta + z_n^{A,B-1} \partial_{q_2} \theta)) \right. \\ \left. - 2 \sum_{j=1}^{\lfloor \frac{n+1-(A+B)}{2} \rfloor} \sum_{\alpha=0}^j \frac{1}{(2i)^j j!} \frac{(A+\alpha)! (B+j-\alpha)!}{A! B!} \right. \\ \left. \times \left(-a_{\alpha_j} y_{n+1-j}^{A+\alpha, B+j-\alpha} + b_{\alpha_j} w_{n+1-j}^{A+\alpha, B+j-\alpha} \right) \right],$$

$$(4.16) \quad 0 = \frac{1}{i} ((\partial_{q_1} z_n^{A-1,B} + \partial_{q_2} z_n^{A,B-1}) + (x_n^{A-1,B} \partial_{q_1} \theta + x_n^{A,B-1} \partial_{q_2} \theta)) \\ - 2 \sum_{j=1}^{\lfloor \frac{n+1-(A+B)}{2} \rfloor} \sum_{\alpha=0}^j \frac{1}{(2i)^j j!} \frac{(A+\alpha)! (B+j-\alpha)!}{A! B!} \\ \times \left(b_{\alpha_j} y_{n+1-j}^{A+\alpha, B+j-\alpha} + a_{\alpha_j} w_{n+1-j}^{A+\alpha, B+j-\alpha} \right),$$

$$(4.17) \quad 0 = \frac{1}{i} ((\partial_{q_1} w_n^{A-1,B} + \partial_{q_2} w_n^{A,B-1}) \\ - 2 \sum_{j=1}^{\lfloor \frac{n+1-(A+B)}{2} \rfloor} \sum_{\alpha=0}^j \frac{1}{(2i)^j j!} \frac{(A+\alpha)!}{A!} \frac{(B+j-\alpha)!}{B!} \\ \times \left(a_{\alpha_j} z_{n+1-j}^{A+\alpha, B+j-\alpha} + b_{\alpha_j} x_{n+1-j}^{A+\alpha, B+j-\alpha} \right)).$$

Proof. We substitute (4.8) into the results of Lemma 4.1 and compare coefficients in powers of p_1, p_2 on either side, using (4.11). \square

As with the coefficients x_n and y_n in (4.1), κ_{n+1}^{\pm} has polynomial form

$$(4.18) \quad \kappa_{n+1}^{\pm}(\mathbf{p}, \mathbf{q}) = \sum_{m=0}^n \sum_{j=0}^m p_1^j p_2^{m-j} \kappa_{n+1}^{(j,m-j)\pm}(\mathbf{q}).$$

Here we apply assumption (A2): $\kappa_{n+1}^{\pm} \approx p_1^n \kappa_{n+1}^{(n,0)\pm}(\mathbf{q})$. In the one dimensional case, this has been shown to be accurate for sufficiently large p , but in practice it holds for much smaller values. By directly constructing the Weyl quantization of $p_1^n \kappa_{n+1}^{(n,0)\pm}(\mathbf{q})$ as in [10, p. 3570], we see that the effect of the coupling operator is negligible outside a small region near the avoided crossing, determined by the small parameter ε which shows that it is reasonable to take the leading term in κ_{n+1}^{\pm} . The two dimensional algebraic differential recursive equations then reduce to the one dimensional case in [10]:

$$(4.19) \quad \begin{aligned} x_{n+1}^{n+1,0} &\approx \frac{i}{2\rho} (\partial_{q_1} y_n^{n,0}), \\ y_{n+1}^{n+1,0} &\approx \frac{i}{2\rho} ((\partial_{q_1} x_n^{n,0})' - (\partial_{q_1} \theta) z_n^{n,0}), \quad 0 \approx \partial_{q_1} z_n^{n,0} + (\partial_{q_1} \theta) x_n^{n,0}. \end{aligned}$$

To ease notation, redefine $x_{n+1} = x_{n+1}^{n+1,0}$, and similarly for y_{n+1}, z_{n+1} . It is unclear what the analogue of (3.1), introduced initially in [6] for the time-adiabatic case, would be for multidimensional systems. We introduce the natural scaling in the first dimension

$$(4.20) \quad \tau(\mathbf{q}) = 2 \int_0^{q_1} \rho(r, q_2) dr.$$

Defining $\tilde{f}(\tau(\mathbf{q})) = f(\mathbf{q})$, the recursive relations (4.19) then become

$$(4.21) \quad \tilde{x}_{n+1}^0 = i \tilde{y}_{n+1}^0, \quad \tilde{y}_{n+1}^0 = i((\tilde{x}_n^0)' + \tilde{\theta}' \tilde{z}_n^0), \quad 0 = (\tilde{z}_n^0)' + \tilde{\theta}' \tilde{x}_n^0,$$

where $\tilde{\theta}' = \frac{d}{d\tau(q_1, q_2)} \tilde{\theta}$. These recursive equations also occur in [11], where they are solved in one dimension, under the assumption that

$$(4.22) \quad \frac{d}{d\tau} \tilde{\theta}(\tau) = \frac{i\gamma}{\tau - \bar{\tau}^{cz}} - \frac{i\gamma}{\tau - \tau^{cz}} + \tilde{\theta}'_r(\tau),$$

where τ^{cz} is a first order complex singularity of $\tilde{\theta}$, and $\tilde{\theta}'_r$ has no singularities closer to the real axis than τ^{cz} . If the avoided crossing occurs at 0, we can write $\rho^2(q) = \delta^2 + g(q)^2$ for some analytic function g such that $g(0) \approx 0$, and g^2 is quadratic in the neighborhood of $q = 0$. Therefore, a Stokes line (i.e., a curve with $\text{Im}(\rho) = 0$)

crosses the real axis perpendicularly [25] and following along this line leads to a pair of complex conjugate points q^{cz}, \bar{q}^{cz} which are complex zeros of ρ . Defining $\tau^{cz} = \tau(q^{cz})$, it is shown in [6] that first order complex singularities of the adiabatic coupling function arise at these complex zeros. This derivation is still valid in our case for each q_2 . The recursive algebraic differential equations solved in [11] then give us κ_n^- to leading order:

(4.23)

$$\kappa_n^-(\mathbf{q}) \approx \kappa_{n,0}^-(\mathbf{q}) := \frac{i^n}{\pi} \rho(\mathbf{q})(n-1)! \left(\frac{i}{(\tau(\mathbf{q}) - \bar{\tau}^{cz}(q_2))^n} - \frac{i}{(\tau(\mathbf{q}) - \tau^{cz}(q_2))^n} \right).$$

It is clear that the results of this section can be extended to higher dimensions by assuming the direction of travel of the wavepacket is in the first dimension. We will now use this observation to design an algorithm for multidimensional transitions using only the one dimensional transition formula.

5. Multidimensional formula derivation. The derivation of a multidimensional formula, under the assumptions above, follows similarly to the one dimensional case. We want to approximate the pseudodifferential operator K_n , which is given by the Weyl quantization of κ_n . The polynomial form of κ_n allows us to simplify the Weyl quantization as follows.

PROPOSITION 5.1. *Let $\kappa(\mathbf{p}, \mathbf{q}) = g(\mathbf{q}) \prod_{i=1}^d p_i^{A_i}$ for $A_i \in \mathbb{N}$. Then*

$$(5.1) \quad (\widehat{\mathcal{W}_\varepsilon \kappa \psi})^\varepsilon(\mathbf{k}) = \frac{1}{(2\pi\varepsilon)^{d/2}} \int_{\mathbb{R}^d} \widehat{g}^\varepsilon(\mathbf{k} - \boldsymbol{\eta}) \prod_{i=1}^d \left(\frac{k_i + \eta_i}{2} \right)^{A_i} \widehat{\psi}^\varepsilon(\boldsymbol{\eta}) d\boldsymbol{\eta}.$$

Proof. The proof is a multidimensional extension of [7, Lemma 4.1]. First, using that $\psi(\mathbf{y}) = (2\pi\varepsilon)^{-d/2} \int_{\mathbb{R}^d} d\boldsymbol{\eta} \widehat{\psi}^\varepsilon(\boldsymbol{\eta}) \exp(i(\boldsymbol{\eta} \cdot \mathbf{y})/\varepsilon)$,

$$\begin{aligned} (\mathcal{W}_\varepsilon \kappa \psi)(\mathbf{x}) &= \frac{1}{(2\pi\varepsilon)^d} \int_{\mathbb{R}^{2d}} d\boldsymbol{\xi} d\mathbf{y} \left(\prod_{i=1}^d \xi_i^{A_i} \right) g\left(\frac{\mathbf{x} + \mathbf{y}}{2}\right) e^{\frac{i}{\varepsilon}(\boldsymbol{\xi} \cdot (\mathbf{x} - \mathbf{y}))} \psi(\mathbf{y}) \\ &= \frac{1}{(2\pi\varepsilon)^{\frac{3d}{2}}} \int_{\mathbb{R}^{3d}} d\boldsymbol{\xi} d\mathbf{y} d\boldsymbol{\eta} \left(\prod_{i=1}^d \xi_i^{A_i} \right) g\left(\frac{\mathbf{x} + \mathbf{y}}{2}\right) e^{\frac{i}{\varepsilon}(\boldsymbol{\xi} \cdot (\mathbf{x} - \mathbf{y}) + \boldsymbol{\eta} \cdot \mathbf{y})} \widehat{\psi}^\varepsilon(\boldsymbol{\eta}). \end{aligned}$$

Now define $\tilde{y}_i = (x_i + y_i)/2$, $i = 1, \dots, d$. Then

$$\begin{aligned} (\mathcal{W}_\varepsilon \kappa \psi)(\mathbf{x}) &= \frac{2^d}{(2\pi\varepsilon)^{\frac{3d}{2}}} \int_{\mathbb{R}^{3d}} d\boldsymbol{\xi} d\tilde{\mathbf{y}} d\boldsymbol{\eta} \left(\prod_{i=1}^d \xi_i^{A_i} \right) g(\tilde{\mathbf{y}}) e^{\frac{i}{\varepsilon}(\boldsymbol{\xi} \cdot \mathbf{x} + (2\tilde{\mathbf{y}} - \mathbf{x}) \cdot (\boldsymbol{\eta} - \boldsymbol{\xi}))} \psi(\boldsymbol{\eta}) \\ &= \frac{2^d}{(2\pi\varepsilon)^d} \int_{\mathbb{R}^{2d}} d\boldsymbol{\xi} d\boldsymbol{\eta} \left(\prod_{i=1}^d \xi_i^{A_i} \right) e^{\frac{i}{\varepsilon}(\boldsymbol{\xi} \cdot (2\boldsymbol{\xi} - \boldsymbol{\eta}))} \psi(\boldsymbol{\eta}) \widehat{g}^\varepsilon(2(\boldsymbol{\xi} - \boldsymbol{\eta})). \end{aligned}$$

We perform a second change of variables $\tilde{\xi}_i = 2\xi_i$ and find that

$$(\mathcal{W}_\varepsilon \kappa \psi)(\mathbf{x}) = \frac{1}{(2\pi\varepsilon)^d} \int_{\mathbb{R}^{2d}} d\tilde{\boldsymbol{\xi}} d\boldsymbol{\eta} \left(\prod_{i=1}^d \left(\frac{\tilde{\xi}_i}{2} \right)^{A_i} \right) e^{\frac{i}{\varepsilon}(\mathbf{x} \cdot (\tilde{\boldsymbol{\xi}} - \boldsymbol{\eta}))} \widehat{\psi}^\varepsilon(\boldsymbol{\eta}) \widehat{g}^\varepsilon(\tilde{\boldsymbol{\xi}} - 2\boldsymbol{\eta}).$$

We apply the scaled Fourier transform to both sides of this equation:

$$\widehat{(\mathcal{W}_\varepsilon \kappa \psi)}^\varepsilon(\mathbf{k}) = \frac{1}{(2\pi\varepsilon)^{\frac{3d}{2}}} \int_{\mathbb{R}^{3d}} d\tilde{\boldsymbol{\xi}} d\boldsymbol{\eta} dx \left(\prod_{i=1}^d \left(\frac{\tilde{\xi}_i}{2} \right)^{A_i} \right) e^{\frac{i}{\varepsilon}(\mathbf{x} \cdot (\tilde{\boldsymbol{\xi}} - \boldsymbol{\eta} - \mathbf{k}))} \hat{\psi}^\varepsilon(\boldsymbol{\eta}) \hat{g}^\varepsilon(\tilde{\boldsymbol{\xi}} - 2\boldsymbol{\eta}).$$

Using that $(2\pi\varepsilon)^{-d} \int dx \exp(i(\mathbf{a} \cdot \mathbf{x})/\varepsilon) = \delta(\mathbf{a})$ allows us to directly compute the \mathbf{x} integral, giving (5.1). \square

Next we linearize the dynamics near the avoided crossing. By (A3), to leading order the uncoupled propagators in (2.16) can be approximated by

$$(5.2) \quad H_1^\pm = -\frac{\varepsilon^2}{2} \nabla_{\mathbf{x}}^2 \pm \delta + \boldsymbol{\lambda} \cdot \mathbf{x}.$$

Then, by the fundamental theorem of calculus,

$$(5.3) \quad e^{\frac{i}{\varepsilon}sH_1^\pm} - e^{\frac{i}{\varepsilon}sH^\pm} = \left\{ \int_0^s e^{\frac{i}{\varepsilon}rH_1^\pm} \left[\frac{i}{\varepsilon}(H_1^\pm - H^\pm) \right] e^{-\frac{i}{\varepsilon}rH^\pm} dr \right\} e^{\frac{i}{\varepsilon}sH^\pm}.$$

Since $H_1^\pm - H^\pm$ is quadratic near zero, the integrand in (5.3) is of order 1 in an $\sqrt{\varepsilon}$ -neighborhood of zero. Outside of this region, the coupling function provides a negligible result, as seen in the one dimensional case [10]. We also use the d -dimensional Avron–Herbst formula [1], which shows that

$$(5.4) \quad e^{-\frac{i}{\varepsilon}s\widehat{H_1^\pm}\varepsilon} = e^{-\frac{i\|\boldsymbol{\lambda}\|^2 s^3}{6\varepsilon}} e^{s(\boldsymbol{\lambda} \cdot \partial_{\mathbf{k}})} e^{-\frac{i}{2\varepsilon}((\|\mathbf{k}\|^2 \pm 2\delta)s - (\boldsymbol{\lambda} \cdot \mathbf{k})s^2)}.$$

Then

$$(5.5) \quad \begin{aligned} \widehat{\psi_n}^\varepsilon(\mathbf{k}, t) &\approx -i\varepsilon^n e^{-\frac{i}{\varepsilon}t\widehat{H^-}\varepsilon} \int_{-\infty}^t e^{-\frac{i\|\boldsymbol{\lambda}\|^2 s^3}{6\varepsilon}} e^{s(\boldsymbol{\lambda} \cdot \partial_{\mathbf{k}})} e^{-\frac{i}{2\varepsilon}((\|\mathbf{k}\|^2 - 2\delta)s - (\boldsymbol{\lambda} \cdot \mathbf{k})s^2)} \widehat{K_{n+1}}^\varepsilon \\ &\quad \times e^{-\frac{i\|\boldsymbol{\lambda}\|^2 s^3}{6\varepsilon}} e^{s(\boldsymbol{\lambda} \cdot \partial_{\mathbf{k}})} e^{-\frac{i}{2\varepsilon}((\|\mathbf{k}\|^2 + 2\delta)s - (\boldsymbol{\lambda} \cdot \mathbf{k})s^2)} \widehat{\phi^+}^\varepsilon(\mathbf{k}) ds. \end{aligned}$$

Using Proposition 5.1 for the coupling function shows that

$$\begin{aligned} \widehat{\psi_n}^\varepsilon(\mathbf{k}, t) &\approx -i \frac{\varepsilon^n}{(2\pi\varepsilon)^{d/2}} e^{-\frac{i}{\varepsilon}t\widehat{H^-}\varepsilon} \int_{-\infty}^t ds e^{-\frac{i\|\boldsymbol{\lambda}\|^2 s^3}{6\varepsilon}} e^{s(\boldsymbol{\lambda} \cdot \partial_{\mathbf{k}})} e^{-\frac{i}{2\varepsilon}((\|\mathbf{k}\|^2 - 2\delta)s - (\boldsymbol{\lambda} \cdot \mathbf{k})s^2)} \\ &\quad \times \int_{\mathbb{R}^d} d\boldsymbol{\eta} \left\{ \sum_{A_i=1, i=1, \dots, d}^{n+1} \widehat{\kappa_{n+1}^{\mathbf{A}, -}}^\varepsilon(\mathbf{k} - \boldsymbol{\eta}) \left(\prod_{i=1}^d \left(\frac{k_i + \eta_i}{2} \right)^{A_i} \right) \right\} \\ &\quad \times e^{-\frac{i\|\boldsymbol{\lambda}\|^2 s^3}{6\varepsilon}} e^{s(\boldsymbol{\lambda} \cdot \partial_{\boldsymbol{\eta}})} e^{-\frac{i}{2\varepsilon}((\|\boldsymbol{\eta}\|^2 + 2\delta)s - (\boldsymbol{\lambda} \cdot \boldsymbol{\eta})s^2)} \widehat{\phi^+}^\varepsilon(\boldsymbol{\eta}), \end{aligned}$$

where $\mathbf{A} = (A_1 \dots A_d)$. The operator $e^{s\boldsymbol{\lambda} \cdot \partial_{\mathbf{k}}}$ is a *shift operator*, and so $e^{s\boldsymbol{\lambda} \cdot \partial_{\mathbf{k}}} f(\mathbf{k}) = f(\mathbf{k} + \boldsymbol{\lambda}s)$. Instead of applying the shift operator to the right, we use the fact that the integral is invariant under the transform $\boldsymbol{\eta} \mapsto \boldsymbol{\eta} - \boldsymbol{\lambda}s$ to apply it to the left: in this case, $f(\boldsymbol{\eta})e^{-s\boldsymbol{\lambda} \cdot \partial_{\boldsymbol{\eta}}} = f(\boldsymbol{\eta} - \boldsymbol{\lambda}s)$. The following transformations take place in the integrand:

$$\begin{aligned} \widehat{\kappa_{n+1}^{\mathbf{A}, -}}^\varepsilon(\mathbf{k} - \boldsymbol{\eta}) &\mapsto \widehat{\kappa_{n+1}^{\mathbf{A}, -}}^\varepsilon(\mathbf{k} - \boldsymbol{\eta}), \quad \mathbf{k} + \boldsymbol{\eta} \mapsto \mathbf{k} + \boldsymbol{\eta} - 2\boldsymbol{\lambda}s, \\ e^{\frac{i}{2\varepsilon}((\|\mathbf{k}\|^2 \pm 2\delta)s - (\boldsymbol{\lambda} \cdot \mathbf{k})s^2)} &\mapsto e^{\frac{i}{2\varepsilon}((\|\mathbf{k} - \boldsymbol{\lambda}s\|^2 \pm 2\delta)s - (\boldsymbol{\lambda} \cdot (\mathbf{k} - \boldsymbol{\lambda}s))s^2)}. \end{aligned}$$

Rearranging gives

$$(5.6) \quad \widehat{\psi_n^-}^\varepsilon(\mathbf{k}, t) \approx -i \frac{\varepsilon^n}{(2\pi\varepsilon)^{d/2}} e^{-\frac{i}{\varepsilon}t\widehat{H^-}^\varepsilon} \\ \times \int_{-\infty}^t \int_{\mathbb{R}^d} ds d\boldsymbol{\eta} \left\{ \sum_{A,B=1}^{n+1} \widehat{\kappa}_{n+1}^{A,-}(\mathbf{k} - \boldsymbol{\eta}) \left(\prod_{i=1}^d \left(\frac{k_i + \eta_i - 2\lambda_i s}{2} \right)^{A_i} \right) \right\} \\ \times \widehat{\phi^+}^\varepsilon(\boldsymbol{\eta}) \exp \left\{ \frac{i}{2\varepsilon} [(\|\mathbf{k}\|^2 - \|\boldsymbol{\eta}\|^2 - 4\delta)s - (\boldsymbol{\lambda} \cdot (\mathbf{k} - \boldsymbol{\eta}))s^2] \right\}.$$

We approximate κ_{n+1}^- with (4.23) and then calculate the scaled Fourier transform:

$$\begin{aligned} \widehat{\kappa_n^-}^\varepsilon(\mathbf{k}) &= \frac{1}{(2\pi\varepsilon)^{d/2}} \int_{\mathbb{R}^d} e^{-(i/\varepsilon)\mathbf{k} \cdot \mathbf{q}} \kappa_n^-(\mathbf{q}) d\mathbf{q} \\ &\approx \frac{(n-1)!}{(2\pi\varepsilon)^{d/2}} \frac{i^n}{\pi} \int_{\mathbb{R}^d} \rho(\mathbf{q}) \left[\frac{i}{(\tau(\mathbf{q}) - \bar{\tau}^{cz}(\mathbf{q}^{d-1}))^n} - \frac{i}{(\tau(\mathbf{q}) - \tau^{cz}(\mathbf{q}^{d-1}))^n} \right] e^{-(i/\varepsilon)\mathbf{k} \cdot \mathbf{q}} d\mathbf{q}, \end{aligned}$$

where $\mathbf{q}^{d-1} = (q_2, \dots, q_d)$. Using (A6), $\rho(\mathbf{q}) \approx \rho(q_1)$, and consequently $\tau(\mathbf{q}) = \tau(q_1)$, $\tau^{cz}(\mathbf{q}^{d-1}) = \tau^{cz}$. Therefore, the Fourier transform in all other dimensions produces a Dirac function, $\frac{1}{\sqrt{2\pi\varepsilon}} \int_{-\infty}^\infty e^{-\frac{ikx}{\varepsilon}} dx = \sqrt{2\pi\varepsilon}\delta(k)$. As $\tau(\mathbf{q}) \approx \tau(q_1)$, we only need to consider the one dimensional case. This is discussed in [10]. A simple extension to d dimensions therefore shows that

$$(5.7) \quad \widehat{\kappa_{n,0}^-}^\varepsilon(\mathbf{k}) = \frac{i}{\sqrt{2\pi\varepsilon}} \left(\frac{k_1}{2\delta\varepsilon} \right)^{n-1} e^{-i\tau_r \frac{k_1}{2\delta\varepsilon}} e^{-\tau_c \frac{|k_1|}{2\delta\varepsilon}} \sqrt{2\pi\varepsilon}^{(d-1)} \delta(k_2, \dots, k_d).$$

We insert (5.7) into (5.6) and rearrange to find that

$$\begin{aligned} \widehat{\psi_n^-}^\varepsilon(\mathbf{k}, t) &= \frac{1}{4\pi\varepsilon} e^{-\frac{i}{\varepsilon}t\widehat{H^-}^\varepsilon} \int_0^\infty ds \int_{\mathbb{R}} d\eta_1 \left(\frac{k_1^2 - \eta_1^2}{4\delta} \right)^n \left(1 - \frac{2\lambda_1 s}{k_1 + \eta_1} \right)^{n+1} \\ &\quad \times e^{-\frac{i\tau_r(k_1 - \eta_1)}{2\delta\varepsilon}} e^{-\frac{\tau_c(|k_1 - \eta_1|)}{2\delta\varepsilon}} \\ &\quad \times \left\{ \int_{\mathbb{R}^{d-1}} d\eta_2 \dots d\eta_d \widehat{\phi^+}^\varepsilon(\boldsymbol{\eta}) e^{\frac{i}{2\varepsilon}[(\|\mathbf{k}\|^2 - \|\boldsymbol{\eta}\|^2)s - \boldsymbol{\lambda} \cdot (\mathbf{k} - \boldsymbol{\eta})s^2]} \delta(k_2 - \eta_2, \dots, k_d - \eta_d) \right\}. \end{aligned}$$

By the identity $f(x) = \int_{-\infty}^\infty \delta(x - a)f(a) da$, the integral in the dimensions $2, \dots, d$ can be evaluated to find that

$$\begin{aligned} \widehat{\psi_n^-}^\varepsilon(\mathbf{k}, t) &= \frac{1}{4\pi\varepsilon} e^{-\frac{i}{\varepsilon}t\widehat{H^-}^\varepsilon} \int_0^\infty ds \int_{\mathbb{R}} d\eta_1 \left(\frac{k_1^2 - \eta_1^2}{4\delta} \right)^n \left(1 - \frac{2\lambda_1 s}{k_1 + \eta_1} \right)^{n+1} \\ &\quad \times e^{-\frac{i\tau_r(k_1 - \eta_1)}{2\delta\varepsilon}} e^{-\frac{\tau_c(|k_1 - \eta_1|)}{2\delta\varepsilon}} \\ &\quad \times \widehat{\phi^+}^\varepsilon(\eta_1, k_2, \dots, k_d) e^{\frac{i}{2\varepsilon}[(|k_1|^2 - |\eta_1|^2 - 4\delta)s - \lambda_1(k_1 - \eta_1)s^2]}. \end{aligned}$$

By (A1), λ_1 is small and hence can be neglected, so that

$$(5.8) \quad \begin{aligned} \widehat{\psi_n^-}^\varepsilon(\mathbf{k}, t) &= \frac{1}{4\pi\varepsilon} e^{-\frac{i}{\varepsilon}t\widehat{H^-}^\varepsilon} \int_0^\infty ds \int_{\mathbb{R}} d\eta \left(\frac{k_1^2 - \eta_1^2}{4\delta} \right)^n e^{-\frac{i\tau_r(k_1 - \eta_1)}{2\delta\varepsilon}} e^{-\frac{\tau_c(|k_1 - \eta_1|)}{2\delta\varepsilon}} \\ &\quad \times \widehat{\phi^+}^\varepsilon(\eta_1, k_2, \dots, k_d) e^{\frac{i}{2\varepsilon}[(|k_1|^2 - |\eta_1|^2 - 4\delta)s]}. \end{aligned}$$

From here we can follow the derivation in [10] and obtain an extension of its main result to d dimensions, given by (2.20). In this derivation, cancelations in the integral remove all dependence on n . Therefore, for implementation of (2.20) we do not need to calculate the pseudodifferential operators K_{n+1}^\pm , or in fact find the optimal choice for n , but we have utilized superadiabatic representations in its construction.

As justification for the proposed algorithm, we note that we evolve the wavepacket on the new potential energy surface, restricted to each strip. As such, we discard any part of the wavepacket that leaves the strip and ignore any additional parts entering from other strips. Since the Schrödinger equation is linear, this introduces two types of error, due to (i) the modification of the potential in each strip, and (ii) the wavepacket broadening out of the selected strip, or into it from the outside. Both errors are small, the first because the strip is quite narrow (so the potential is approximately constant) and the second because the time for which we actually evolve is small (of the order of the crossing region in the optimal superadiabatic basis).

In practice, for the examples in section 6, we compute the BOA dynamics on a uniform two dimensional grid. Once the center of mass of the wavepacket reaches the avoided crossing, we interpolate the wavepacket onto a grid with the new p_1 direction parallel to that of \mathbf{p}_{COM} . Instead of treating strips of the appropriate width, we simply apply the formula (2.20) along each of the one dimensional lines parallel to p_1 (or \mathbf{p}_{COM}); this reduces to applying the one dimensional formula. For small ε , this is essentially equivalent to the algorithm above, as the approximate potentials of neighboring lines are very similar and the evolution time in the optimal superadiabatic basis is very short.

6. Numerical results. We perform the algorithm on a selection of examples, and compare it to the two-level “exact” computation, where the Strang splitting method is used. For all examples, we consider two wavepackets given in momentum space by

$$(6.1) \quad \widehat{\psi}_0^\varepsilon(\mathbf{p}) = \frac{1}{N_\psi} \exp\left(-\frac{\|\mathbf{p} - \mathbf{p}_0\|^2}{2\varepsilon}\right) \exp\left(-i\frac{(\mathbf{p} - \mathbf{p}_0) \cdot \mathbf{x}_0}{\varepsilon}\right),$$

$$(6.2) \quad \widehat{\phi}^\varepsilon(\mathbf{p}) = \frac{1}{N_\phi} \exp\left(-\frac{\|\mathbf{p} - \mathbf{p}_0\|^6}{2\varepsilon}\right) \exp\left(-i\frac{(\mathbf{p} - \mathbf{p}_0) \cdot \mathbf{x}_0}{\varepsilon}\right),$$

where N_α are normalization constants. To ensure that the wavepacket has sufficient momentum to travel through the avoided crossing, we choose to define the wavepackets at the avoided crossing point, and then evolve backwards in time away from the avoided crossing using one-level dynamics, before evolving forwards and applying the formula. In practice, the initial wavepacket can be given in any initial location, provided it is far enough from the avoided crossing to be unaffected by coupling effects.

To compare the formula results to exact calculations, we use the L^2 -relative error

$$(6.3) \quad Er_{\text{rel}}(\psi_1, \psi_2) = \max\left(\frac{\|\psi_1 \pm \psi_2\|}{\|\psi_1\|}, \frac{\|\psi_1 \pm \psi_2\|}{\|\psi_2\|}\right),$$

where $\|\cdot\|$ is the standard L^2 -norm. For comparison to other algorithms which do not calculate phase, it is also beneficial to consider the relative absolute error

$$(6.4) \quad Er_{\text{abs}}(\psi_1, \psi_2) = \max\left(\frac{\||\psi_1| - |\psi_2|\|}{\|\psi_1\|}, \frac{\||\psi_1| - |\psi_2|\|}{\|\psi_2\|}\right)$$

or the relative mass error

$$(6.5) \quad Er_{\text{mass}}(\psi_1, \psi_2) = \max \left(\frac{\|\psi_1\|}{\|\psi_2\|}, \frac{\|\psi_2\|}{\|\psi_1\|} \right) - 1.$$

Example 6.1. Consider the diabatic potential matrix

$$(6.6) \quad V(\mathbf{x}) = \begin{pmatrix} \tanh(x_1) & \delta \\ \delta & -\tanh(x_1) \end{pmatrix}.$$

This is a direct extension of a one dimensional problem, and as there is no dependence in x_2 , the assumptions made in the derivation in section 5 are exactly valid if the direction of the wavepacket is independent of p_2 . The lower surface is given by $V_L = -V_U$. The upper adiabatic surface is shown in Figure 3a. We take parameters

$$(6.7) \quad \{\varepsilon, \delta, \mathbf{p}_0, \mathbf{x}_0\} = \left\{ \frac{1}{30}, \frac{1}{2}, (6, 1), (0, 0) \right\}.$$

Using a mesh of $2^{13} \times 2^{13}$ points on the domain $[-20, 20]^2$, starting at time 0, we evolve the wavepacket back to time -2 with time-step $1/(50\|\mathbf{p}_0\|)$ and then evolve forwards to time 2, applying the algorithm, and compare to the exact calculation. For the Gaussian wavepacket ψ , $Er_{\text{rel}} = 0.0151$, $Er_{\text{abs}} = 0.0151$, and $Er_{\text{mass}} = 0.0016$. For non-Gaussian ϕ , $Er_{\text{rel}} = 0.0389$, $Er_{\text{abs}} = 0.0387$, and $Er_{\text{mass}} = 0.0023$. The result of the formula and the corresponding error are shown in Figures 4 and 5.

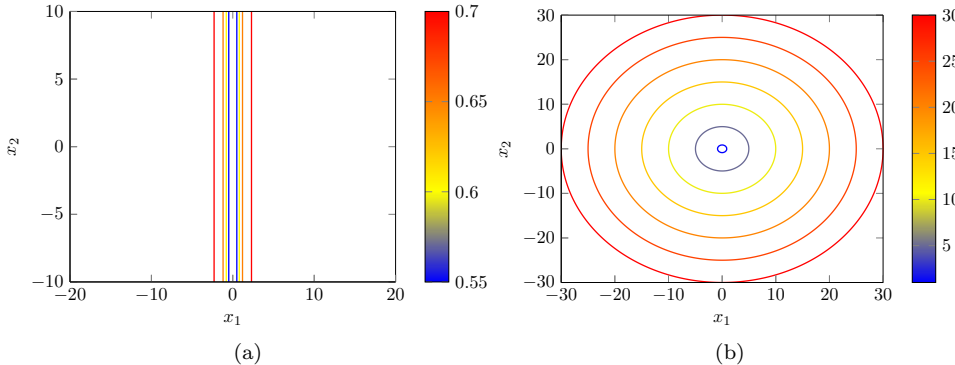


FIG. 3. Contour plot of the upper adiabatic potential surfaces for Example 6.1 (left) and Example 6.2 (right). In these examples, $V_U = -V_L$.

Example 6.2. We consider the diabatic potential matrix described in [14]

$$(6.8) \quad V(\mathbf{x}) = \begin{pmatrix} x_1 & \sqrt{x_2^2 + \delta^2} \\ \sqrt{x_2^2 + \delta^2} & -x_1 \end{pmatrix},$$

which is a modified Jahn–Teller diabatic potential, where the conical intersection is replaced with an avoided crossing with gap 2δ . The upper adiabatic surface is shown in Figure 3b. We use parameters

$$(6.9) \quad \{\varepsilon, \delta, \mathbf{p}_0, \mathbf{x}_0\} = \left\{ \frac{1}{30}, 0.5, (5, 2), (0, 0) \right\}.$$

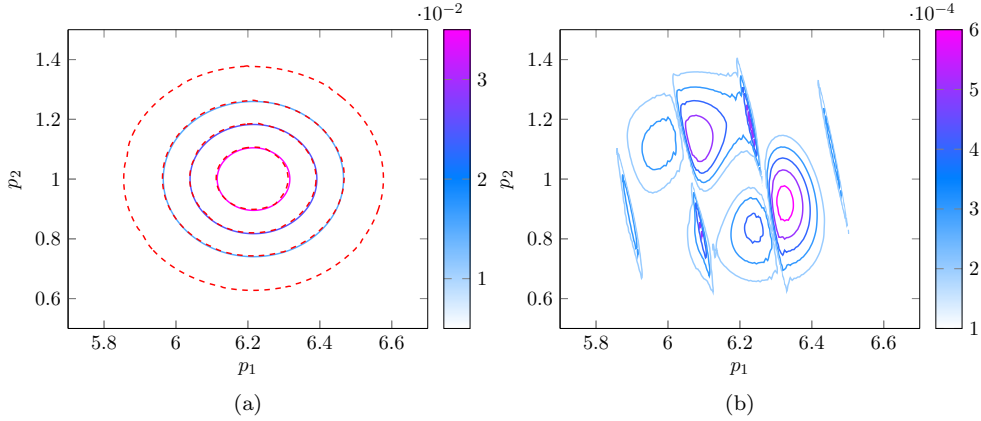


FIG. 4. Results for Example 6.1 when using parameters in (6.7) with an initial wavepacket of form (6.1). Left: exact calculation (solid line) versus formula result (dashed line). Contours for the formula result are at the same values as the neighboring exact contours. Right: relative error.

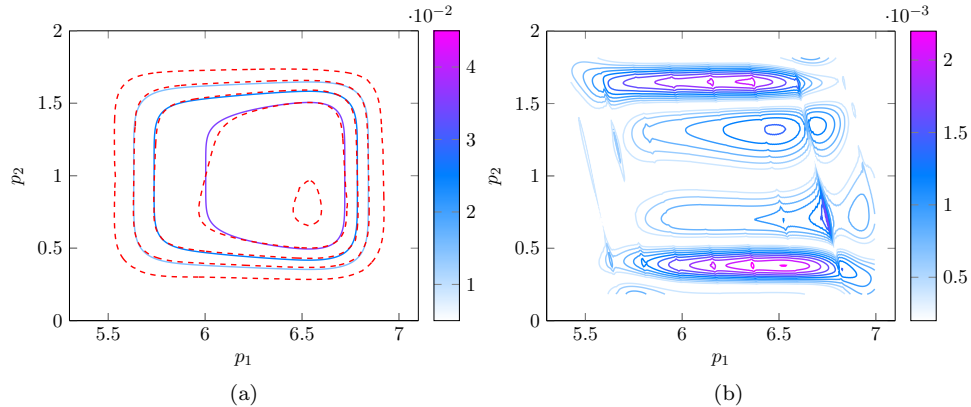


FIG. 5. As in Figure 4 but with initial wavepacket (6.2).

Using a mesh of $2^{13} \times 2^{13}$ points on the domain $[-40, 40]^2$, we start at time 0 and evolve backwards with time-step $1/(50\|\mathbf{p}_0\|)$ to time $-20/\|\mathbf{p}_0\|^2$, and then forwards to time $20/\|\mathbf{p}_0\|^2$, finding that $Er_{rel} = 0.0351$, $Er_{abs} = 0.0304$, and $Er_{mass} = 0.0029$ using Gaussian initial wavepacket ψ_0 and $Er_{rel} = 0.0679$, $Er_{abs} = 0.0616$, and $Er_{mass} = 0.0033$ for non-Gaussian initial wavepacket ϕ . Figures 6 and 7 display the result of the formula compared to the exact calculation. We now use the parameters

$$(6.10) \quad \{\varepsilon, \delta, \mathbf{p}_0, \mathbf{x}_0\} = \left\{ \frac{1}{30}, 0, (5, 0), (0, 0.5) \right\}.$$

In addition, we included the sign of x_2 in the off-diagonal elements of $V(\mathbf{x})$, which then gives the standard Jahn-Teller Hamiltonian. However, let us stress that nonadiabatic transitions must be exactly the same for the Hamiltonian with and without the sign included. The reason is that by that choice, we have just chosen a different diabatic representation, but the (unique) adiabatic representation remains the same. It is an advantage of our method, which only uses the adiabatic energy

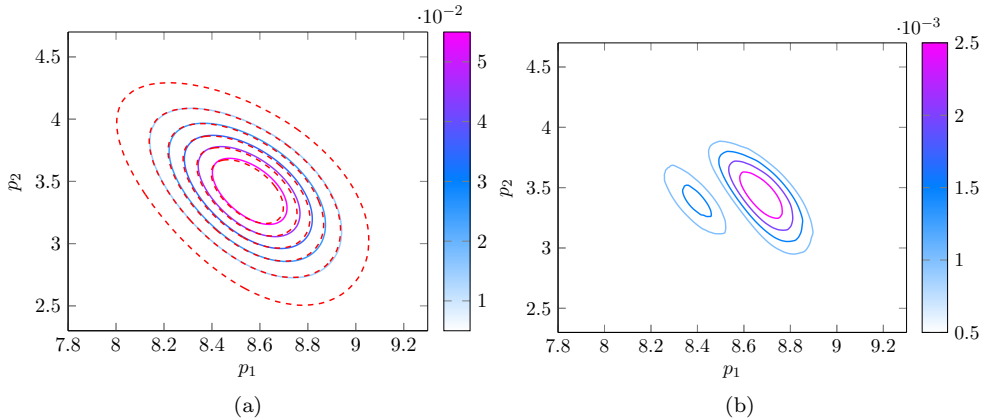


FIG. 6. Results for Example 6.2 when using parameters in (6.9) with initial wavepackets of form (6.1). Results are presented as in Figure 4.

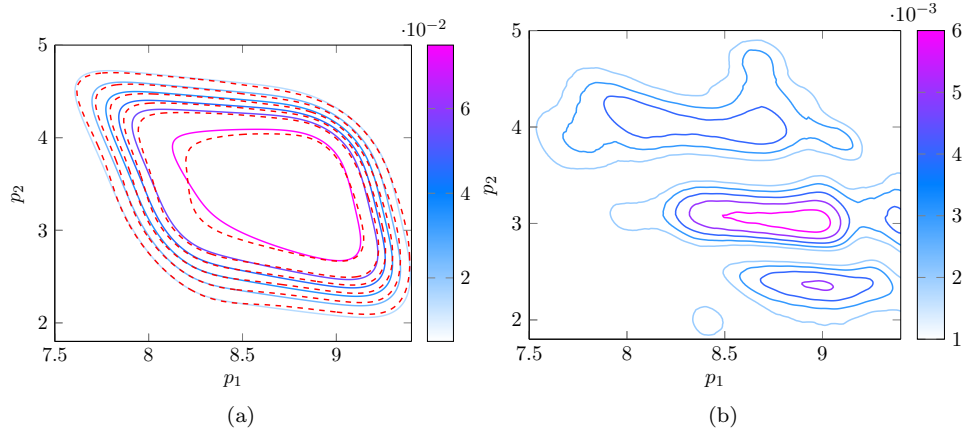


FIG. 7. As in Figure 6 but with initial wavepacket (6.2).

surfaces, that it is insensitive to such a change. The Jahn–Teller Hamiltonian has a conical intersection. We have chosen momentum such that the center of mass of the wavepacket does not cross the intersection. We evolve back to $-25/\|p_0\|^2$ with a time-step of $1/(50\|p_0\|)$, evolve forwards to $25/\|p_0\|^2$ using the algorithm, and compare with the exact calculation. Then $Er_{\text{rel}} = 0.0638$, $Er_{\text{abs}} = 0.0550$, and $Er_{\text{mass}} = 0.0309$ for an initial wavepacket of form ψ_0 and $Er_{\text{rel}} = 0.1511$, $Er_{\text{abs}} = 0.0850$, and $Er_{\text{mass}} = 0.0604$ for ϕ ; the transmitted wavepacket and error are given in Figure 8. Although the relative error is large in this final calculation, the absolute error and mass error show that the algorithm has performed well, given that it is not designed for systems where δ is small or vanishing. Figure 9 also shows that the shape of the wavepacket is still well approximated qualitatively.

We note that the relative and absolute errors in Example 6.2 differ, while in Example 6.1 they are the same. We believe this is due to a change in phase when ρ is not flat in q_2 , and so the error due to the modification of the potential surface for each strip is larger.

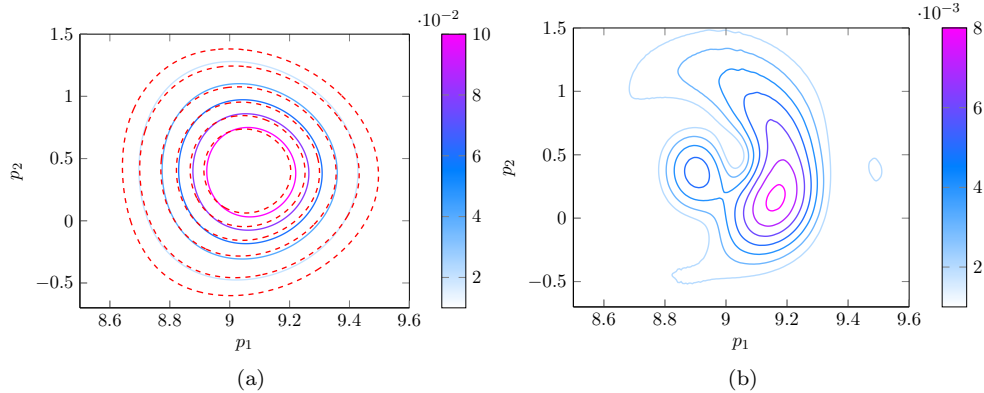


FIG. 8. As in Figure 6 but with parameters (6.10).

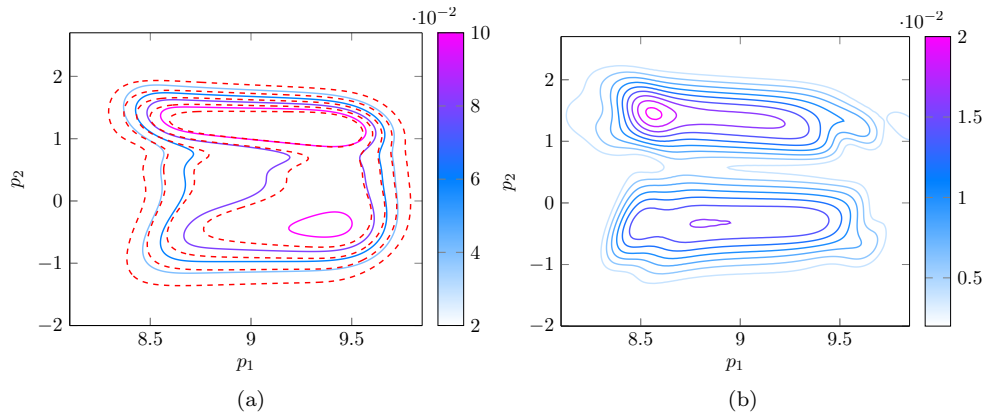


FIG. 9. As in Figure 8 but with initial wavepacket (6.2).

7. Conclusions and future work. In this paper, we have constructed an algorithm which can be used to approximate the transmitted wavepacket in nonadiabatic transitions in multiple dimensions, by constructing a formula based on the one dimensional result in [7], and appealing to the linearity of the Schrödinger equation to decompose the dynamics onto strips with potentials that are constant in all but one direction. Presented examples in two dimensions show similar accuracy to one dimensional analogues, and are accurate in the phase, which is beyond the capability of standard surface hopping models.

Correctly approximating the phase of the wavepacket becomes important when more than one transition takes place. In [20], various one dimensional examples of multiple transitions are explored using the formula, with accurate results. In future work, we will consider multiple transitions in two dimensions using the algorithm. This will involve taking into account the effect of geometric phase [12] due to multiple avoided crossings, as well as constructing an approximation of the wavepacket which remains on the upper level after a transition has taken place. We also will compare the results of the algorithm considered in this paper with other algorithms designed to approximate nonadiabatic transitions; see, e.g., [19].

Acknowledgment. We wish to thank the anonymous referees for their careful reading of the manuscript and suggestions which have helped to improve it.

REFERENCES

- [1] J. AVRON AND I. HERBST, *Spectral and scattering theory of Schrödinger operators related to the Stark effect*, Comm. Math. Phys., 52 (1977), pp. 239–254.
- [2] A. BACH, *An Introduction to Semiclassical and Microlocal Analysis*, 1st ed., Springer, New York, 2002.
- [3] A. BELYAEV, W. DOMCKE, C. LASSE, AND G. TRIGILA, *Nonadiabatic nuclear dynamics of the ammonia cation studied by surface hopping classical trajectory calculations*, J. Chem. Phys., 142 (2015), 104307.
- [4] A. BELYAEV, C. LASSE, AND G. TRIGILA, *Landau-Zener type surface hopping algorithms*, J. Chem. Phys., 140 (2014), 224108.
- [5] M. BERRY, *Histories of adiabatic quantum transitions*, Proc. Roy. Soc. London Ser. A, 429 (1990), pp. 61–72.
- [6] M. BERRY AND R. LIM, *Universal transition prefactors derived by superadiabatic renormalization*, J. Phys. A, 26 (1993), pp. 4737–4747.
- [7] V. BETZ AND B. GODDARD, *Accurate prediction of nonadiabatic transitions through avoided crossings*, Phys. Rev. Lett., 103 (2009), 213001.
- [8] V. BETZ AND B. D. GODDARD, *Nonadiabatic transitions through tilted avoided crossings*, SIAM J. Sci. Comput., 33 (2011), pp. 2247–2276, <https://doi.org/10.1137/100802347>.
- [9] V. BETZ, B. GODDARD, AND U. MANTHE, *Wave packet dynamics in the optimal superadiabatic approximation*, J. Chem. Phys., 144 (2016), 224109.
- [10] V. BETZ, B. GODDARD, AND S. TEUFEL, *Superadiabatic transitions in quantum molecular dynamics*, Proc. R. Soc. Lond. Ser. A Math. Phys. Eng. Sci., 465 (2009), pp. 3553–3580.
- [11] V. BETZ AND S. TEUFEL, *Precise coupling terms in adiabatic quantum evolution*, Ann. Henri Poincaré, 6 (2005), pp. 217–246.
- [12] A. BOHM, A. MOSTAFAZADEH, H. KOIZUMI, Q. NIU, AND J. ZWANZIGER, *The Geometric Phase in Quantum Systems*, Texts Monogr. Phys., Springer, Heidelberg, 2003.
- [13] M. BORN AND R. OPPENHEIMER, *Zur Quantentheorie der Moleküle*, Ann. Phys. (Leipzig), 84 (1927), pp. 457–484.
- [14] L. CHAI, S. JIN, Q. LI, AND O. MORANDI, *A multiband semiclassical model for surface hopping quantum dynamics*, Multiscale Model. Simul., 13 (2015), pp. 205–230, <https://doi.org/10.1137/140967842>.
- [15] W. DOMCKE, D. YARKONY, AND K. HORST, *Conical Intersections: Electronic Structure, Dynamics and Spectroscopy*, Adv. Phys. Chem. 15, World Scientific, Singapore, 2004.
- [16] W. DOMCKE, D. YARKONY, AND K. KÖPPEL, *Conical Intersections: Theory, Computation and Experiment*, Adv. Chem. Phys. 17, World Scientific, Singapore, 2011.
- [17] E. FABIANO, G. GROENHOF, AND W. THIEL, *Approximate switching algorithms for trajectory surface hopping*, Chem. Phys., 351 (2008), pp. 111–116.
- [18] C. FERMANIAN KAMMERER AND C. LASSE, *Single switch surface hopping for molecular dynamics with transitions*, J. Chem. Phys., 128 (2008), 144102.
- [19] C. FERMANIAN KAMMERER AND C. LASSE, *An Egorov theorem for avoided crossings of eigenvalue surfaces*, Comm. Math. Phys., 353 (2017), pp. 1011–1057.
- [20] B. GODDARD AND T. HURST, *Multiple Superadiabatic Transitions and the Landau-Zener Formula*, preprint, <https://arxiv.org/abs/1804.04660>, 2018.
- [21] V. N. GORSHKOV, S. TRETIAK, AND D. MOZYRSKY, *Semiclassical Monte-Carlo approach for modelling non-adiabatic dynamics in extended molecules*, Nat. Commun., 4 (2013), 2144.
- [22] G. A. HAGEDORN AND A. JOYE, *Molecular propagation through small avoided crossings of electron energy levels*, Rev. Math. Phys., 11 (1999), pp. 41–101.
- [23] S. HAMMES-SCHIFFER AND J. TULLY, *Proton transfer in solution: Molecular dynamics with quantum transitions*, J. Chem. Phys., 101 (1994), pp. 4657–4667.
- [24] I. HORENKO, C. SALZMANN, B. SCHMIDT, AND C. SCHÜTTE, *Quantum-classical Liouville approach to molecular dynamics: Surface hopping Gaussian phase-space packets*, J. Chem. Phys., 117 (2002), pp. 11075–11088.
- [25] A. JOYE, G. MILETI, AND C. PFISTER, *Interferences in adiabatic transition probabilities mediated by Stokes lines*, Phys. Rev. A, 44 (1991), pp. 4280–4295.
- [26] R. KAPRAL, *Surface hopping from the perspective of quantum-classical Liouville dynamics*, Chem. Phys., 481 (2016), pp. 77–83.
- [27] R. KAPRAL AND G. CICCOTTI, *Mixed quantum-classical dynamics*, J. Chem. Phys., 110 (1999),

- pp. 8919–8929.
- [28] T. KATSAOUNIS AND I. KYZA, *A posteriori error control and adaptivity for Crank–Nicolson finite element approximations for the linear Schrödinger equation*, Numer. Math., 129 (2015), pp. 55–90.
 - [29] P. KUNTZ, J. KENDRICK, AND W. WHITTON, *Surface-hopping trajectory calculations of collision-induced dissociation processes with and without charge transfer*, Chem. Phys., 38 (1979), pp. 147–160.
 - [30] L. LANDAU, *Collected Papers of L.D. Landau*, Pergamon Press, Oxford, UK, 1965.
 - [31] C. LASSEUR AND T. SWART, *Single switch surface hopping for a model of pyrazine*, J. Chem. Phys., 129 (2008), 034302.
 - [32] J. LU AND Z. ZHOU, *Frozen Gaussian approximation with surface hopping for mixed quantum-classical dynamics: A mathematical justification of fewest switches surface hopping algorithms*, Math. Comp., 87 (2018), pp. 2189–2232.
 - [33] W. MILLER AND T. GEORGE, *Semiclassical theory of electronic transitions in low energy atomic and molecular collisions involving several nuclear degrees of freedom*, J. Chem. Phys., 56 (1972), pp. 5637–5652.
 - [34] U. MÜLLER AND G. STOCK, *Surface-hopping modeling of photoinduced relaxation dynamics on coupled potential-energy surfaces*, J. Chem. Phys., 107 (1997), pp. 6230–6245.
 - [35] H. NAKAMURA, *Nonadiabatic Transition: Concepts, Basic Theories and Applications*, World Scientific, Singapore, 2012.
 - [36] V. ROUSSE, *Landau–Zener transitions for eigenvalue avoided crossings in the adiabatic and Born–Oppenheimer approximations*, Asymptot. Anal., 37 (2004), pp. 293–328.
 - [37] J. STINE AND J. MUCKERMAN, *On the multidimensional surface intersection problem and classical trajectory “surface hopping,”* J. Chem. Phys., 65 (1976), pp. 3975–3984.
 - [38] S. TEUFEL, *Adiabatic Perturbation Theory in Quantum Dynamics*, Springer, Berlin, Heidelberg, 2003.
 - [39] J. TULLY, *Molecular dynamics with electronic transitions*, J. Chem. Phys., 93 (1990), pp. 1061–1071.
 - [40] J. TULLY, *Perspective: Nonadiabatic dynamics theory*, J. Chem. Phys., 137 (2012), 22A301.
 - [41] J. TULLY AND R. PRESTON, *Trajectory surface hopping approach to nonadiabatic molecular collisions: The reaction of H+ with D2*, J. Chem. Phys., 55 (1971), pp. 562–572.
 - [42] D. ZENER, *Non-adiabatic crossings of energy levels*, Proc. R. Soc. Lond. A, 137 (1932), pp. 696–702.